

REMARKS

Reconsideration is requested.

Claims 1, 2, 4-8 and 10-17 are pending. Claims 1, 2, 4-8, 9-14, 16 and 17 are indicated as containing allowable subject matter. See page 4 of the Office Action dated October 18, 2010. Claim 9 was canceled, without prejudice, in the Amendment filed August 2, 2010.

The claims have been amended, without prejudice. Support for the revisions may be found throughout the specification. Claim 15 has been revised to include the structural component also described in claim 1, from which claim 15 continues to depend. The revisions to the claims do not raise new issues requiring further search and/or consideration.

The lamellar crystallographic structure of the metal chalcogenide allows it to exist in the form of nanoboxes made up of closed, generally hollow rectangular parallelepipeds (i.e., MX_2 lamellar material can fold onto itself to spontaneously form a hollow rectangular parallelepiped-shaped nanobox during the process of formation).

The objection to claim 16 will be obviated by entry of the present Amendment. Entry of the Amendment and withdrawal of the objection are requested.

Claim 1 has been revised according to the Examiner's helpful suggestion, and claim 15 has been revised, without prejudice, to obviate the Section 112, second paragraph, rejection of claims 1, 2, 4-8 and 9-17¹. The applicants submit that metals from Group IV, such as Sn and Pb can form compounds of formula MX_2 having a

¹ As noted above, claim 9 was canceled earlier in prosecution.

lamellar crystallographic structure. Filed concurrently herewith are the following documents in support of same:

Yujie et al, Journal of Physics: Condensed Matter, 2003, 15, L661-L665;

Liu et al, Materials Letters 63 (2009) pp 512-514;

Silverman, Inorganic Chemistry, 1966, 5(11) pp 2067-2069.

SnS_2 , PbS_2 , SnSe_2 and PbSe_2 are all metal chalcogenides having a lamellar crystallographic structure and having the formula MX_2 . Claim 15 is submitted to be definite. Entry of the present Amendment and withdrawal of the rejection are requested.

To the extent not obviated by the above amendments, the Section 102 rejection of claim 15 over Suzuki (U.S. Patent Application Publication No. 2003/0191222 A1) is traversed. Reconsideration and withdrawal of the rejection are requested in view of the above and the following distinguishing comments.

The cited art does not teach nanoparticles having the form of a hollow nanobox. The cited art further fails to teach that the metal chalcogenide has a lamellar crystallographic structure. Withdrawal of the Section 102 rejection is requested.

Ordinary skill will appreciate that any compound having a cubic, tetragonal or orthorhombic crystallographic structure can form nanocrystals having a rectangular parallelepiped shape (i.e., a solid rectangular parallelepiped, where the inside of the rectangular parallelepiped is completely filled with the compound lattice structure).

Claim 15 does not relate however to solid rectangular parallelepiped-shaped nanoparticles. Rather, the claim is directed to metal chalcogenide nanoparticles of

formula MX_2 having the form of nanoboxes made up of closed, generally hollow rectangular parallelepipeds.

The claimed process involves a method for preparing closed-structure nanoparticles of metal chalcogenides having a lamellar crystallographic structure. During this process, a lamellar sheet of such a metal chalcogenide can spontaneously fold onto itself to form a closed hollow structure. When the metal chalcogenide is MX_2 , as defined in claim 15, the closed structure can have the form of nanoboxes made up of closed, generally hollow rectangular parallelepipeds. These hollow rectangular parallelepiped-shaped nanoparticles are the object of claim 15.

The cited art fails to teach generally *hollow* rectangular parallelepipeds of the rejected claim. Withdrawal of the Section 102 rejection is requested.

Moreover, the applicants submit that the only metal chalcogenides of formula MX_2 that the cited reference discloses are the following oxides: titania (TiO_2), and zirconia (ZrO_2). See ¶[0048]. Suzuki also discloses alumina (Al_2O_3) and silica (SiO_2).

The applicants submit however that silica is not a metal according to the rejected claim. Aluminum is not a transition metal or a metal of group IV. Furthermore, Al_2O_3 is not a metal chalcogenide of formula MX_2 . With respect to titania and zirconia, while Ti and Zr are transition metals, TiO_2 and ZrO_2 do not have a lamellar or layered crystallographic structure. See attached pages of "Advanced Inorganic Chemistry" by Cotton, Wilkinson, Murillo and Bochmann, 6th edition, Wiley ("Titanium compounds" on pages 697-698 which discusses TiO_2 as compared with discussion of TiS_2 ("Titanium disulfide, like disulfides of Zr, Hf, V, Nb and Ta, has a layer structure."); "Zirconium

oxides and mixed oxides" on page 882 which describes ZrO_2 as compared to "the other chalcogenides ZrE_2 and HfE_2 ($\text{E}=\text{S}, \text{Se}, \text{Te}$) have layered structures and are intrinsic semiconductors. They can form intercalation compounds which generally have layered structures."). TiO_2 (titania) and ZrO_2 (zirconia) will be recognized therefore as metal chalcogenides that do not exist in a lamellar crystallographic structure.

Additional evidence that TiO_2 and ZrO_2 do not have a lamellar crystallographic structure relates to the hardness of these materials as compared to layered materials. Specifically, compounds having a lamellar crystallographic structure contain weak cohesive forces (Van der Waals) between the structural layers which allow sliding over each other (strong cohesion forces within the sheet/layer are secured by covalent or ionic bonds). As a result, lamellar materials (such as graphite, talc, MoS_2 , mica, etc.) have a low hardness, and are for example used for solid lubrication (MoS_2).

In stark contrast, TiO_2 and ZrO_2 belong to the class of ceramics, and are therefore known for their hardness. The comparison is demonstrated in the following Table.

		Mohs hardness	Absolute hardness
Ceramics	ZrO ₂	6.5 - 7.0	200 - 400
	TiO ₂	6.0 - 6.5	70 - 100
	SiO ₂ (quartz)	7.0	100
	Al ₂ O ₃	9	400
Lamellar compounds	MoS₂	1-2	1-2
	Mg₃Si₄O₁₀(OH)₂ (<i>tal</i>c)	1	1
	Graphite	1-2	1-2

TiO₂ and ZrO₂ are ceramic-type materials that exhibit high strength, high fracture toughness, excellent wear resistance and high hardness. As a result of these properties, the applicants submit that titania and zirconia are typically used as orthopaedic implants and dental ceramics, for example.

In stark contrast, lamellar compounds are not hard materials and they contain weak cohesion forces between layers. The applications of lamellar compounds (e.g., lubrication materials) are far different from those of ceramic materials such as titania and zirconia. TiO₂ and ZrO₂ are not lamellar crystallographic structured materials.

The cited art describes TiO₂ and ZrO₂ in ¶[0048]), and metal oxide particles having a rectangular parallelepiped shape in a separate, independent paragraph (¶[0053]).

Notwithstanding the facts that TiO₂ and ZrO₂ do not exist in lamellar crystallographic structure, and that the rectangular parallelepipeds in the cited art are not hollow, there is no description in the cited art of "rectangular parallelepiped shape"

BASTIDE et al.
Appl. No. 10/581,342
Atny. Ref.: 5006-10
Amendment After Final Rejection
December 17, 2010

being associated with TiO_2 and ZrO_2 . Accordingly, the applicants submit that the cited art does not amount to a description of, for example, nanoparticles of a metal chalcogenide MX_2 of the rejected claim in the form of rectangular parallelepipeds.

The cited art fails to teach or describe the claimed invention and withdrawal of the Section 102 rejection is requested.

The claims are submitted to be in condition for allowance a Notice to that effect is requested. The Examiner is requested to contact the undersigned, preferably by telephone, in the event anything further is required in this regard.

Respectfully submitted,

NIXON & VANDERHYTE P.C.

By: /B. J. Sadoff/
 B. J. Sadoff
 Reg. No. 36,663

BJS:
901 North Glebe Road, 11th Floor
Arlington, VA 22203-1808
Telephone: (703) 816-4000
Facsimile: (703) 816-4100

from the plot of $\log \frac{1}{2}K(1/T)$, yields a straight line which intercepts the origin of the Cartesian axes. If it is assumed that the dominant contribution to Q_1/Q_2 comes only from the single Cu-Cu stretching vibration, ν_1 , then

$$Q_1/Q_2 = \frac{\{1 - \exp(-h\nu_1/kT)\}}{\{1 - \exp(-h\nu_2/kT)\}} \quad (10)$$

The Cu-Cu stretching mode, ν_2 , appears to be about 1.6 times higher in frequency than ν_1 , since as $T \rightarrow \infty$, $\log(Q_1/Q_2) \rightarrow \log(\nu_2/\nu_1) \approx 0.2$. As an illustrative calculation, we take $\nu_2 = 100 \text{ cm}^{-1}$ and $\nu_1 = 63 \text{ cm}^{-1}$ to obtain the correction curve given in the lower part of Figure 2. The order of magnitude of the Cu-Cu vibrational correction is, in fact, sufficient to yield the expected intercept for the $\log \frac{1}{2}K(1/T)$ plot (see dashed line of Figure 2). A necessary consequence of the correction is a slightly diminished value of $J = 840 \text{ cal mole}^{-1}$ (i.e., $-2J_{12} = 294 \text{ cm}^{-1}$).

CONTRIBUTION FROM DEPARTMENT OF RESEARCH AND
 DEVELOPMENT, PENNSALT CHEMICALS CORPORATION,
 KING OF PRUSSIA, PENNSYLVANIA

High-Pressure (70-kbar) Synthesis of New Crystalline Lead Dichalcogenides

By MEYER S. SHAFERMAN

Received June 5, 1968

By subjecting mixtures of the elements or of lead monochalcogenides with excess sulfur and selenium to temperatures of 800–2400° and pressures of 20–70 kbars, we have synthesized the stable crystalline compositions PbSe_2 , PbSSe , and two polymorphs of PbS_2 , one of the latter appearing to be isomorphous with SnS_2 . Until now, only crystalline PbS , PbSe , PbS - PbSe , or amorphous polysulfides and polyselenides had been reported.

Experimental Section

Starting materials consisted of compressed pellets of 99.9+ % lead, 99.999+ % sulfur, and 99+ % selenium prepared at ambient conditions with chalcogenide:lead ratios of at least 3:1. Also pellets composed of mixtures of $\text{PbS} + \text{S}$, $\text{PbS} + \text{PbSe} + \text{S} + \text{Se}$, and $\text{PbSe} + \text{Se}$ in ratios of 1:2, 1:1:2:2, and 1:2 were used in tetrahedral pyrophyllite sample holders with graphite heating elements described previously.¹ Thin-walled boron nitride sleeves were used to insulate the reaction mixture from the heater. A tetrahedral anvil apparatus of National Bureau of Standards design² was used for all syntheses. Discussion of temperature and pressure calibrations and experimental procedure have been reported earlier.³

- (1) H. T. Hall, *Science*, **128**, 440 (1958).
- (2) E. C. Lloyd, U. O. Hutton, and D. P. Johnson, *J. Res. Natl. Bur. Std.*, **C68**, 69 (1969).
- (3) J. R. Seulen and M. S. Silverman, *J. Polym. Sci.*, **A1**, 823 (1963).

Results and Discussion

Duncan and Ott⁴ reported the synthesis and isolation of an amorphous lead disulfide which was quite unstable at ambient conditions. We have prepared two crystalline polymorphs of lead disulfide from elemental and $\text{PbS} + \text{S}$ mixtures. One of these was prepared repeatedly at 20 kbars and 1600–1800°. Each time this synthesis was carried out, an explosion or blowout occurred so that the quantity of gray-black solid remaining in the sample cavity was sufficient only for X-ray characterization. The complete X-ray powder diffraction pattern we obtained for this product, which we shall call $\alpha\text{-PbS}_2$, is shown in Table I. As indicated,

TABLE I
X-RAY POWDER DIFFRACTION PATTERNS

hkl	SnS_2^a		$\alpha\text{-PbS}_2^b$		J^c
	d, Å	l	Obsd	Calcd	
001	5.9	50	6.0	5.9	s
100	3.15	40			
101	2.78	100	2.85	2.83	s
102	2.14	50	2.13	2.18	m
110	1.82	50			
111	1.74	40			
103	1.66	13	1.68	1.67	s
201	1.52	20			
202	1.394	13			
113	1.334	10			
210	1.192	4	1.23	1.22	m
211	1.170	13			
114	1.146	8	1.16	1.18	w

^a ASTM 1-1010. ^b Cu $K\alpha$ radiation taken as 1.5418 Å. ^c Visually estimated.

the material appears to be isostructural with the CdI_2 -type SnS_2 structure. The calculated lattice constants for $\alpha\text{-PbS}_2$ based on hexagonal indexing are $a = 3.89$, $c = 5.91$ Å. These constants seem reasonable when compared to the reported values $a = 3.63$ and $c = 5.86$ Å for the tin sulfide,⁵ which would be expected to occupy a smaller volume than PbS_2 considering the relative sizes of tin and lead radii. When we tried thicker BN capsules, Ni reaction vessels, or substituted pulse heating to maintain the reaction conditions without blowouts, we obtained either PbS or Ni_3PbS_2 as the only products indicated by X-ray analyses.

The other crystalline products were prepared from Pb-S , Pb-S-Se , and Pb-Se elemental mixtures in atomic ratios of 1:3, 1:1.5:1.5, and 1:4, respectively. Successful syntheses were also carried out with mixtures of the monochalcogenides and excess sulfur and/or selenium. The strongest lines of the X-ray powder diffraction patterns obtained for these are listed in Table II. The patterns could be indexed on the basis of a tetragonal KN_3 structure type with average lattice constants as follows: $\beta\text{-PbS}_2$, $a = 6.10 \pm 0.10$, $c = 7.48 \pm 0.10$ Å; PbSSe , $a = 6.27 \pm 0.01$, $c = 7.57 \pm 0.02$ Å; and PbSe_2 , $a = 6.36 \pm 0.08$, $c = 7.63 \pm 0.10$ Å. The increasing lattice constants with increasing

- (4) W. E. Duncan and E. Ott, *J. Am. Chem. Soc.*, **62**, 3010 (1941).
- (5) R. W. G. Wyckoff, "The Structure of Crystals," 2nd ed. The Chemical Catalog Co., Inc., New York, N. Y., 1931, p. 239.

TABLE II
 X-RAY POWDER DIFFRACTION PATTERNS

<i>hkl</i>	β -PbS ₂		PbSSe		PbSe	
	<i>d</i> , Å ^a	<i>I</i> ^b	<i>d</i> , Å	<i>I</i>	<i>d</i> , Å	<i>I</i>
110	4.30	75	4.14	60	4.56	60
111	3.73	25	3.79	25	3.86	10
200	3.07	50	3.15	60	3.22	50
112	2.83	100	2.80	100	2.91	100
211	2.58	5	2.63	50	2.70	50
202	2.38	50	2.42	60	2.47	60
220	2.17	25	2.22	50	2.27	25
310	1.93	50	1.98	60	2.04	60
222	1.87	60	1.91 ^c	50	1.96	25
004	1.87	25	1.92 ^c	50
312	1.72	60	1.75	50	1.79	25
114	1.77	10
321	1.65	5	1.70	25	1.74	25
204	1.60	25	1.62	50	1.65	25
330	1.44	10	1.48	10
402	1.45 ^c	50	1.48	50
323, 224	1.41	50	1.47	25
NI ^d	1.40	10
420	1.305	5	1.338	25
332	1.345	50	1.375 ^e	50	1.407	25
314	1.353	10	1.397	50
NI	1.337	10	1.357	10
422	1.280	25	1.316	25	1.346	25
510	1.200	25	1.231	25	1.261	25

^a Copper K α radiation taken as 1.5418 Å. KCl internal standard used for all; however, only intensities were corrected for KCl presence. ^b The intensities of the diffraction lines were measured as peak heights above background using a densitometer. They are expressed as percentages of the intensity of the strongest line. ^c Broad line. ^d Not indexed.

selenium content are consistent with the relative atomic sizes of S and Se. The measured densities were 5.51 g/cc for β -PbS₂ and 7.48 g/cc for PbSe₂ compared to 6.47, 7.15, and 7.80 g/cc calculated for four molecules per unit cell for PbS₂, PbSSe, and PbSe₂ respectively.

Conditions favorable for at least partial conversion to the tetragonal dichalcogenides were found to be above 30 kbars and 650° in most cases. At 45 kbars, 1500°, essentially quantitative conversions were obtained in 5 min. Microscopic examination of the homogeneous products revealed charcoal-gray, elongated, rodlike crystals usually radiating toward the center of the reaction pellet. No β -PbS₂ was found below 600° and only PbS formed between 10 and 30 kbars and 600 and 1200°. PbSe₂ and PbSSe also required temperatures above 500–600° for their formation. Excess sulfur was removed by successive washings with CS₂ followed by ether rinsing and vacuum drying. An aqueous solution of 10% Na₂S separated elemental Se from the selenide without decomposing the lead compound, as indicated by the X-ray pattern of the dried solute.

Anal. Calcd for β -PbS₂: Pb, 76.4; S, 23.6. Found: Pb, 71.8, 74.1; S, 27.2, 24.7. Calcd for PbSSe: Pb, 65.1; S, 10.1; Se, 24.8. Found: Pb, 58.3; S, 10.5; Se, 25.2. Calcd for PbSe₂: Pb, 56.7; Se, 43.3. Found: Pb, 57.6, 51.1, 55.2; Se, 42.4 (by difference), 45.1, 44.8 (by difference).

Since the change in *d* spacings shown in Table II

for each *hkl* value is nearly linearly related to composition, possibly there exists a whole solid solution range of compositions such as PbS_{2-x}Se_x where *x* varies from 0 to 2. Our attempts to prepare the intermediate compositions Pb₂S₃Se and Pb₂Se₃S from the appropriate atomic ratio mixtures containing excess S and Se, however, yielded only PbS and PbSe, respectively, plus a few unidentified lines, according to the X-ray patterns.

Thermogravimetric analysis (tga) of purified β -PbS₂ in pure, dry O₂ showed a weight gain of 12.8% compared to 11.7% calculated for oxidation of the disulfide to PbSO₄. The residue had an X-ray powder diffraction pattern characteristic of PbSO₄ plus a few weak unidentified lines. The initial weight gain started at 235° and leveled off at 462°. In N₂, β -PbS₂ showed an initial weight loss at 150° leveling off at 317°. The reaction, purposely interrupted at the first plateau in the tga curve, yielded PbS only. This mode of decomposition is typical of group IVa disulfides and was also the same for PbSSe and PbSe₂, which decomposed initially to PbS-PbSe and PbSe, respectively. The weight loss of the diselenide began at 344° and leveled off at 513°.

The distinct differences between β -PbS₂ reported here and the lead disulfide reported by Duncan and Ott⁴ are as follows: (1) Weak PbS lines only were present on their original X-ray films from fresh samples and this pattern became more intense as samples were exposed. The products we obtained including the mixed selenide and diselenide showed no trace of the monochalcogenide X-ray powder patterns after 8 months of storage at room temperature. (2) The density of their amorphous product increased from 4.47 to 5.40 g/cc after air exposure for 1 week (6.8 g/cc is the calculated density of a PbS-S 1:1 mixture). In the same period of time the density of β -PbS₂, 5.51 g/cc, was virtually unchanged. (3) Tetragonal β -PbS₂ analyzed close to this stoichiometry after air exposure for 1 week, whereas the amorphous disulfide decomposed to PbS_{1.4} after remaining at ambient conditions overnight. (4) Duncan and Ott reported that some decomposition took place at temperatures as low as 50° in contrast to our tga results mentioned previously. (5) The color of all of our lead products was charcoal-gray, whereas most of the amorphous disulfides were maroon or reddish brown, although a few were reported to be black.

Some preliminary electrical resistance measurements were taken with increasing pressure from 10 to 70 kbars on PbSe₂. No significant changes were observed, indicating that the basic character of the compound is covalent. Chemical behavior of the tetragonal disulfide was as follows: no reaction in water or ethanol, partial solubility in 0.1 *N* NaOH, vigorous reaction in concentrated HCl with H₂S evolution, and immediate reaction in concentrated HNO₃ to yield a precipitate. Tetragonal PbSe₂ did not superconduct above 0.3°K,⁶ the lowest temperature at which tests were run.

(6) D. B. McWhan, private communication.

Vol. 5, No. 11, November 1966

NOTES 2069

Acknowledgments.—The author thanks Dr. J. R. Soulen for helpful suggestions and discussion, Mr. E. A. Bruce and Mr. W. S. Garrison for experimental assistance, Dr. W. Clavan and Mr. R. F. Hamilton for obtaining the X-ray patterns, Dr. D. B. McWhan of Bell Laboratories for the superconductivity test, and the analytical and shop groups for their help. This work was supported in part by the Office of Naval Research and the U. S. Army Research Office (Durham).

CONTRIBUTION FROM THE DEPARTMENT OF PHYSICAL
 SCIENCES, UNIVERSITY OF IDAHO, MOSCOW, IDAHO 83843

Fluorine-19 Chemical Shifts in Nuclear Magnetic Resonance Spectra of Fluorosulfate-Containing Compounds

By FREDERICK A. HONORST AND JEAN'NE M. SHREEVE

Received June 13, 1966

Since the synthesis of peroxydisulfuryl difluoride ($S_2O_8F_2$) by Dudley and Cady,¹ the number of compounds containing the fluorosulfate group, OSO_2F , has increased rapidly inasmuch as reactions of the former or its derivatives provide a facile route to the introduction of this group into fluoroolefins and simple inorganic molecules. In characterizing some of these fluorosulfates, the chemical shift of the fluorine bonded to sulfur was reported with respect to an internal or an external standard. The literature reports no attempts to compare the magnitudes of the chemical shifts as a function of chemical or molecular environment. However, it has been stated that resonances in the -50-ppm region are diagnostic of the fluorine in fluorosulfate since the frequency in organic molecules seems to be relatively constant.² In order to study this relationship, several of these compounds have been synthesized and their nuclear magnetic resonance spectra have been measured with trichlorofluoromethane as the internal reference.

Experimental Section

The compounds examined were prepared through the use of conventional methods. A Varian Model 4311B high-resolution spectrometer equipped with a 40-Mc oscillator was used to determine the nuclear magnetic resonance spectra. Reproducibility of chemical shift values was about ± 0.1 ppm for consecutive measurements on the same or different preparations of a compound or for measurements separated by 24 hr. The samples were contained in sealed 5-mm o.d. Pyrex tubes heated to 35° prior to use to check pressure stability. Roughly 50% solutions (by volume) were prepared with CCl_3F , which had been dried over P_2O_5 , as the reference compound. In the case of $HOSO_2F$, because of immiscibility with CCl_3F , an external reference was used. CCl_3F was sealed into a 2-mm o.d. tube, and this was placed in the liquid $HOSO_2F$. External references were also used with $ClOSO_2F$ and $BrOSO_2F$.

(1) R. B. Dudley and G. H. Cady, *J. Am. Chem. Soc.*, **79**, 513 (1957).
 (2) M. Lustig, *Inorg. Chem.*, **4**, 1838 (1965).

In Table I, the fluorosulfate compounds are listed with the respective chemical shifts given in ppm.

TABLE I
 F^{19} CHEMICAL SHIFTS OF OSO_2F IN FLUOROSULFATE-CONTAINING
 COMPOUNDS RELATIVE TO CCl_3F

Compound	Shift, ppm	Compound	Shift, ppm
$ClOSO_2F^a$	-33.9 ^b	$PO_2SO_2O_2F^b$	-48.8
$POSO_2F^b$	-28.3	$CF_3(OSO_2F)^c$	-48.7
CF_3OSO_2F	-27.9	$C_2F_5OSO_2F^a$	-49.0
$PO_2SO_2O_2F^b$	-40.4	$O_2S(OSO_2F)_2$	-48.5
$BrOSO_2F$	-41.3 ^b	$NF_2CF_2CF_2OSO_2F^f$	-60.4
$FOOSO_2F^b$	-42.6	$C_2F_5(OSO_2F)_2$	-50.7
NF_2OSO_2F	-44.1	$CF_3CF_2CF_2CF_2(OSO_2F)CF_3^g$	-51.0
CF_3OSO_2F	-46.8	$CF_3CF_2CF_2(OSO_2F)CF_3^g$	-51.2
$CF_3C(O)OSO_2F^{d,e}$	-47.4	$HOSO_2F$	-65.8 ^b
$CClFOSO_2F^d$	-48.0		

^{a, c, e} For comparison with previously reported shifts, consult the following: (a) W. P. Gilbreath and G. H. Cady, *Inorg. Chem.*, **2**, 496 (1963); (b) G. Franz and F. Neumayr, *ibid.*, **3**, 521 (1964); (c) J. J. Delfino and J. M. Shreeve, *ibid.*, **5**, 308 (1966); (d) D. D. DesMarceau and G. H. Cady, *ibid.*, **5**, 169 (1966); (e) see ref 2; (f) M. Lustig and J. K. Ruff, *Inorg. Chem.*, **4**, 1441 (1965); (g) B. L. Earl, B. K. Hill, and J. M. Shreeve, *ibid.*, in press. ^b External reference.

Although the observed shifts as a function of the substituent group cannot be simply related to any single factor, the data, in general, appear to be internally consistent, which makes some interesting comparisons possible. (1) Introduction of CF_3 group(s) shifts resonances to lower field: $POSO_2F > CF_3OSO_2F > C_2F_5OSO_2F$; $ClOSO_2F > CClF_2OSO_2F$; $PO_2SO_2O_2F > PO_2SO_2CF_2OSO_2F > PO_2SO_2C_2F_5OSO_2F$; $NF_2OSO_2F > NF_2C_2F_5OSO_2F$. (2) Substitution of SO_2F for fluorine shifts to lower field: $PO_2SO_2SO_2F > PO_2SO_2SO_2C_2F_5OSO_2F$; $CF_3OSO_2F > PO_2SO_2CF_2OSO_2F$; $POSO_2F > PO_2SO_2O_2F$. (3) Substitution of a halogen or pseudo-halogen for a fluorine may shift to lower field: $CF_3OSO_2F > CClF_2OSO_2F$; $FOOSO_2F > NF_2OSO_2F$; $FOSO_2F > BrOSO_2F$; or to higher field: $FOSO_2F < ClOSO_2F$. (4) Introduction of an oxygen atom varies: $POSO_2F > FOOSO_2F$, while $CF_3OSO_2F < CF_3FOOSO_2F$.

Acknowledgment.—The support of this work by the National Science Foundation is gratefully acknowledged. We are indebted to Mr. B. J. Nist of the University of Washington for running the nmr spectra.

CONTRIBUTION FROM THE INSTITUTE
 OF INORGANIC CHEMISTRY,
 UNIVERSITY OF WÜRZBURG, WÜRZBURG, GERMANY

Trimethylsiloxydimethylgold

By ROBERT SCHMIDBAUER AND MANFRED BERGHAID

Received June 13, 1966

We wish to report the synthesis of trimethylsiloxydimethylgold, a heterosiloxane species¹ containing the Si-O-Au linkage.

Trimethylgold, prepared according to a method described by Gilman and Woods,² was converted to

(1) H. Schmidbauer, *Angew. Chem.*, **77**, 205 (1955); *Angew. Chem. Intern. Ed. Engl.*, **4**, 201 (1965).
 (2) H. Gilman and L. A. Woods, *J. Am. Chem. Soc.*, **70**, 550 (1948).



Synthesis and characterization of SnSe₂ hexagonal nanoflakes

Kegao Liu^{a,b}, Hong Liu^{b,*}, Jiyang Wang^{b,*}, Liming Feng^a

^a School of Materials Science and Engineering, Shandong Jianzhu University, Fengning Road, Jinan 250010, China

^b State Key Laboratory of Crystal Materials, Shandong University, 27 Shandong Road, Jinan 250001, China

ARTICLE INFO

Article history:
 Received 28 August 2008
 Accepted 23 October 2008
 Available online 6 November 2008

Keywords:
 Crystal growth
 Nanomaterials
 Semiconductors
 SnSe₂

ABSTRACT

Single phase SnSe₂ was synthesized at 180 °C by hydrothermal co-reduction method from SnCl₄·2H₂O and SeO₂. Its morphology and growth direction were investigated. The products were characterized by X-ray diffraction (XRD), transmission electron microscopy (TEM) and field emission scanning electron microscope (FESEM). Experimental results show that, the SnSe₂ powder almost consists of regular and homogeneous hexagonal nanoflakes which grow along (1001) crystal plane, these nanoflakes are about 300–700 nm in side length and 30–40 nm in thickness.

© 2008 Elsevier B.V. All rights reserved.

1. Introduction

Tin selenides such as SnSe and SnSe₂ have brilliant application prospects due to their excellent optical and electrical properties, which can be applied in film electrodes [1], infrared optoelectronic devices, thermoelectric refrigerators and solar cells etc [2]. Therefore there have been many research works about tin selenides in recent past, such as nanocrystalline SnSe synthesized by Qian's group from aqueous solution [3,4], SnSe nanowires prepared via an ethylenediamine-assisted polyol route [5], plate like and rod like orthorhombic SnSe crystals grown by an organic solution method [6], nanocrystalline photoconducting SnSe thin films with quantum dots prepared by a chemical bath deposition method [7], Sn–Se compounds on a gold electrode fabricated by electrochemical atomic layer epitaxy [8], SnSe single crystals grown by a direct vapour transport technique [9] and nanocrystalline tin selenides synthesized by electron beam irradiation method [10]. The petal-like nanoflakes and irregular sheet-like SnSe₂ have been synthesized via the solvothermal route [11]. While hexagonal nanoflakes of SnSe₂ were successfully synthesized by hydrothermal method in this work.

2. Experimental details

For preparing SnSe₂, 0.002 mol SnCl₄·2H₂O and 0.004 mol SeO₂ were added into a stainless steel autoclave with a Teflon liner of 20 ml capacity. The autoclave was filled with deionized water up to 80% of the total volume. After ultrasonic agitation for about 30 min, 2 ml hydrazine hydrate (N₂H₄·H₂O) was poured into the reactants. The autoclave was sealed and heated at temperature 180 °C for 24 h in an electric furnace. After heating, it was cooled down to room

temperature naturally. The black product was collected by filtration, washed with deionized water and absolute ethanol, and then dried at 60 °C as per reference [12].

The powder samples obtained were analyzed by X-ray diffraction (XRD) on a D/Max-γ A model (Japan Rigaku) XRD system with Ni-filtered Cu Kα (λ = 1.5059 Å). The size and morphology of the product powders were observed by a model JEM-100CXII transmission electron microscope (TEM) and a model JSM-6700F field emission scanning electron microscope (FESEM).

3. Results and discussion

3.1. Synthesis of SnSe₂ by hydrothermal co-reduction

Fig. 1 shows the XRD pattern of the product prepared by hydrothermal co-reduction method at 180 °C. It shows that the major phase in the product is SnSe₂.

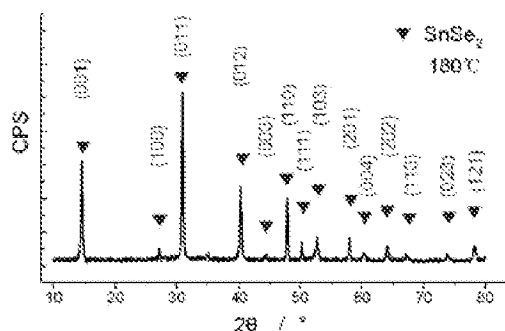


Fig. 1. The XRD pattern of the powder prepared by hydrothermal method.

* Corresponding authors. Tel.: +86 53188362807.

E-mail addresses: hongliu@sdu.edu.cn (H. Liu), jywang@sdu.edu.cn (J. Wang).

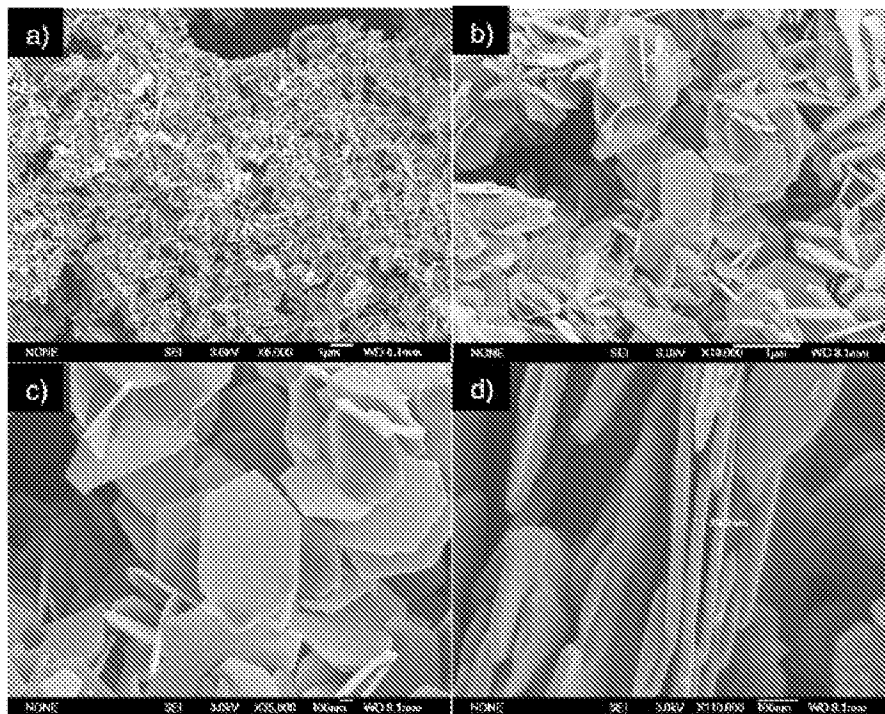
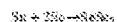
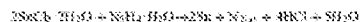
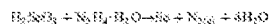
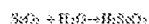


Fig. 2. SEM images of SnSe_2 synthesized at 180°C .

The reaction mechanism is proposed as follows: When all the reactants are put into the autoclave and heated, Sn^{4+} and Se^{6+} are easily reduced by hydrogen decomposed from $\text{NH}_4\text{H}_2\text{Se}$ because their positive electrode potential are much higher than hydrogen. The as-reduced Sn atoms and Se atoms are very active and can easily combine to be SnSe_2 molecules [32]. The reaction processes which can be proved possible by above XRD result are as follows.



3.2. The morphology of SnSe_2 powders

Fig. 2 shows the SEM images of SnSe_2 synthesized at 180°C . Fig. 2a indicates that the SnSe_2 powder is flake like. Some hexagonal flakes can be found in Fig. 2b at higher

magnification. Fig. 2c and d indicate that the SnSe_2 powder almost consists of regular and homogenous hexagonal nanoflakes, which are about 600–700 nm in side length and 30–40 nm in thickness.

Fig. 3 shows the TEM image of SnSe_2 hexagonal flakes which grow along (0001) crystal plane according to electron diffraction spots of a flake in Fig. 3b. The flake nucleus grows along the (100) plane and forms flake-like tiny crystals because of its layered growth habit and the weak bonding among layers. Since the reaction temperature is low, the formation rate of SnSe_2 molecules and the growth rate of the crystal are low. Therefore it is easy to get small crystalline nanoflakes with well-formed hexagonal morphology [32,33].

4. Conclusions

Single phase SnSe_2 was synthesized at 180°C by hydrothermal co-reduction method from $\text{SnCl}_4 \cdot 2\text{H}_2\text{O}$ and SeO_2 . The SnSe_2 powder almost consists of regular and homogenous hexagonal nanoflakes which grow along the (0001) crystal plane, these nanoflakes are about 600–700 nm in side length and 30–40 nm in thickness.

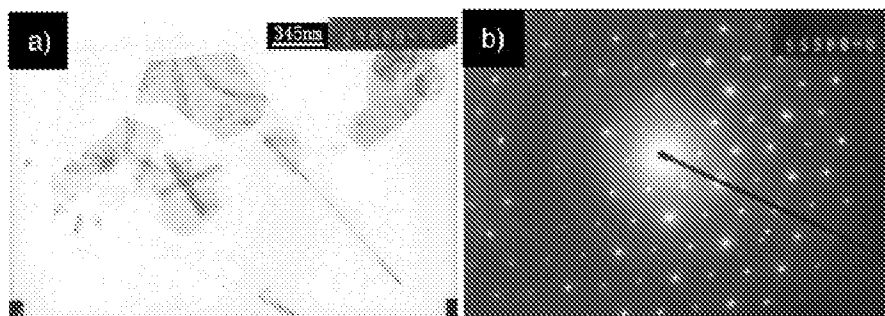


Fig. 3. TEM images of SnSe_2 synthesized at 180°C .

Acknowledgement

This work was supported by the Shandong excellent middle-aged and Young scientist encourage and reward foundation (No. 2006RS04017).

References

- [1] Xue BZH, Cheng SCB, Yao J, Fu ZHW. *Acta Phys.-Chim. Sin.* 2006;22(7):583–7. In Chinese.
- [2] Han QJ, Zou Y, Liu XR, Yang SL. *Chinese J. Org. Chem.* 2005;21(11):1740–3.
- [3] Wang WGN, Gong Y, Qian YT. *Mater Res Bull.* 1999;34:403–6.
- [4] Zhang WK, Yang ZH, Liu JW, Qian YT. *J. Cryst. Growth* 2008;317:157–60.
- [5] Shen GZH, Chen B, Yang KB. *J. Chem. Lett.* 2003;32:426–7.
- [6] Han ZHB, Li YH, Yu QHM, Zhang CB, Chen XY, Zhao HJ, et al. *J. Cryst. Growth* 2001;228:1–5.
- [7] Pejova B, Grizdanov E. *Thin Solid Films* 2007;515:5205–11.
- [8] Qiao ZHF, Zhang WC, Wang CHB. *J. Electroanal. Chem.* 2005;538:171–6.
- [9] Ajay A, Chaki Smiti B, Lakshminarayana D. *Mater Lett* 2007;61:5188–90.
- [10] Li ZH, Jiao ZH, Wu MH, Liu Q. *Colloids Surf A Physicochem Eng Asp* 2008;313–314:40–2.
- [11] Peng HR, Huang J. *J. Qingdao Univ. Sci Technol* 2005;27(3):422–30.
- [12] Cui HM, Liu H, Li X, Wang JW. *J. Solid State Chem* 2004;177:4001–6.
- [13] Dobrova E, Yatchew R. *J. Mater. Sci.* 1990;31:3647–9.

LETTER TO THE EDITOR

Single-crystalline SnS_2 nano-belts fabricated by a novel hydrothermal method

Yujie Ji, Hui Zhang, Xiangyang Ma, Jin Xu and Deren Yang[†]

State Key Lab of Silicon Materials, Zhejiang University, Hangzhou 310027,
People's Republic of China

E-mail: wseyang@sil.zju.edu.cn

Received 5 September 2003

Published 24 October 2003

Online at stacks.iop.org/JPhysCM/15/L661

Abstract

SnS_2 nano-belts have been prepared by a novel thioglycolic acid (TGA) assisted hydrothermal method. X-ray diffraction reveals that the SnS_2 nano-belts are of hexagonal structure and well crystallized. Transmission electron microscopy observation shows that the SnS_2 nano-belts have a width of 80–160 nm and a length of up to several micrometres, and high-resolution transmission electron microscopy further identifies that the SnS_2 nano-belts are single-crystalline in nature. A preliminary mechanism for the TGA-assisted hydrothermal synthesis of SnS_2 nano-belts is presented.

1. Introduction

SnS_2 belongs to the interesting class of isomorphous materials that are in many ways between two-dimensional (layer type) systems and three-dimensional crystals, and exhibits a strong anisotropy of optical properties [1]. SnS_2 is a lamellar structure semiconductor with a band gap of about 2.35 eV [2] and therefore has the potential to act as an efficient solar cell material [3]. It is also of interest in holographic recording systems and electrical switching [4, 5].

Traditional methods for the preparation of tin sulfides include chemical vapour deposition [6, 7], electrochemical deposition [8], molecular beam epitaxy (MBE) [9] and spray pyrolysis [10]. However, all these reported methods require either a relatively high reaction temperature (more than 300 °C) or expensive instruments. Furthermore, over the past decade, the synthesis and functionalization of one-dimensional nano-structure materials has become one of the most highly active research areas [11–13]. Qian's groups have developed a mild solvothermal route to synthesize both SnS_2 nanocrystals [14] and belt-like SnS_2 crystals [15], but this method uses toxic, dangerous and expensive solvents. Here, we report the synthesis of SnS_2 nano-belts by a novel thioglycolic acid (TGA) assisted hydrothermal method which

[†] Author to whom any correspondence should be addressed.

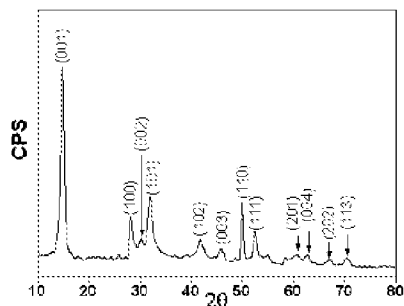


Figure 1. XRD pattern of the SnS_2 nano-belts prepared by the TGA-assisted hydrothermal method.

is milder, simpler, more practical and less harmful to the environment than the solvothermal method.

2. Experiment

All chemicals are analytical grade without further purification. First, 0.001 mol $\text{SnCl}_2 \cdot 2\text{H}_2\text{O}$ powder, 50 μL TGA, and 100 ml of Na_2S with a concentration of 0.04 M were placed into a beaker. After stirring, the reactants were put into a Teflon-lined autoclave of 150 ml capacity, which was filled with deionized water up to 80% of the total volume. Next, the autoclave was maintained at 200 °C for 20 h, then cooled to room temperature naturally. The mixture turned black due to the formation of SnS_2 precipitates. The products were filtered out, washed with alcohol and deionized water several times and then dried at 60 °C for 30 min.

An x-ray diffraction (XRD) pattern was obtained on a Rigaku D/max-ga x-ray diffractometer with graphite monochromatized $\text{Cu K}\alpha$ radiation ($\lambda = 1.54178 \text{ \AA}$). Transmission electron microscopy (TEM) observation was performed on a Philips CM200 high-resolution transmission electron microscope with an accelerating voltage of 200 kV.

3. Results and discussion

All the peaks in the XRD pattern (figure 1) can be indexed to the hexagonal structure of SnS_2 with lattice constants $a = 3.648$, $c = 5.899 \text{ \AA}$, in good agreement with JCPDS No 23-0677. XRD analysis detected no impurities such as SnO_2 . The strong and sharp diffraction peaks suggest that the products are well crystallized.

Typical TEM images of as-prepared samples are shown in figure 2. This figure clearly reveals the belt-like morphology of the SnS_2 nanocrystals with a width of 80–160 nm and a length of up to several micrometers. The selected area electron diffraction (SAED) pattern confirms that the as-synthesized nano-belts consist of SnS_2 , and reveals their single-crystal nature. Additional structural characterization of the SnS_2 nano-belts was carried out using a high-resolution transmission electron microscope (HRTEM). Figure 3 shows a typical HRTEM image of a SnS_2 nano-belt. The image clearly shows that fringes with a lattice spacing of about 0.315 nm can be found, which corresponds to {100} planes of SnS_2 .

The energy dispersive x-ray (EDX) spectrum of the individual SnS_2 nano-belt shown in figure 2 is given in figure 4. The very strong peaks related to Sn and S are found in the spectrum.



Figure 2. TEM images of multi SnS₂ nano-belts. The upper right inset corresponds to the SAED pattern of the SnS₂ nano-belts, the lower right inset corresponds to the TEM image of an individual SnS₂ nano-belt.

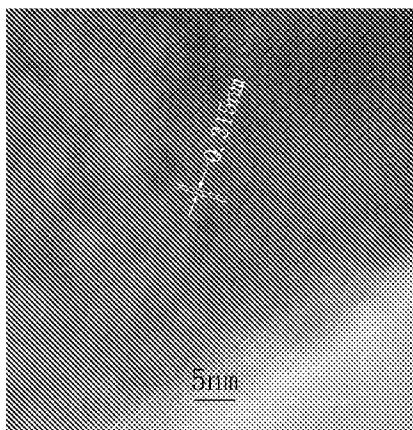
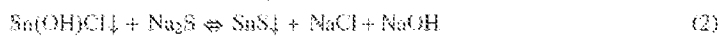


Figure 3. HRTEM image of a SnS₂ nano-belt.

The very weak O peak may originate from the oxidation of SnS₂ nano-belts exposed to the air. The C and Cu peaks come from the copper grid used to support the samples.

Previously, TGA was widely used as a stability agent preventing nano-crystals from aggregating [16, 17]. In our synthetic route, TGA is critical for the formation of the belt-like structure. The detailed mechanism can be expressed as follows.



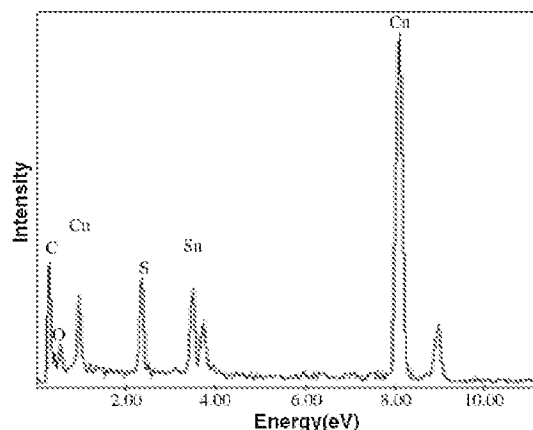
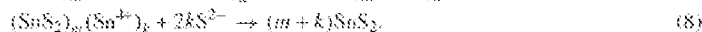
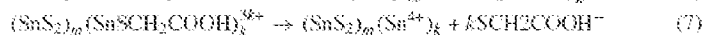
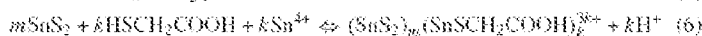


Figure 4. EDX spectrum of the individual SnS₂ nano-belt shown in figure 2.



Prior to the hydrothermal process, the hydrolysis of SnCl₂ and the formation of SnS nuclei were carried out via reactions (1) and (2). Due to the instability of SnS and the excess of S²⁻, SnS₂ nuclei were formed in the hydrothermal process according to reactions (3)–(5). Compared with the conventional hydrothermal process, in the TGA-assisted hydrothermal process the marked difference is the formation of (SnS₂)_m(SnSCH₂COOH)_k^{3k+} complex clusters in the solution via reaction (6). Reaction (7) represents the dissociation of SCH₂COOH⁻ from the SnS₂ complex clusters. We believe that the dissociation of SCH₂COOH⁻ occurs in a local region of the complexed SnS₂ cluster, where there are Sn⁴⁺ exposed to the S²⁻ existing in the solution. Therefore, during the hydrothermal process, the formation of SnS₂ proceeds along specific directions. However, the exact mechanism for the formation of SnS₂ nano-belts in the TGA-assisted hydrothermal process is still under investigation by our group. Other quasi one-dimensional chalcogenides, such as CdS, Bi₂S₃ and PbS, have been prepared following the basic idea behind the hydrothermal process introduced in this paper has been reported [18, 19].

4. Conclusion

Single-crystalline SnS₂ nano-belts have been successfully prepared by a TGA-assisted hydrothermal method, with the advantages of simplicity, cost-effectiveness and reduced environmental impact. The growth mechanism of SnS₂ nano-belts has been discussed and the effect of TGA proposed. Furthermore, it is reasonable to believe that the TGA-assisted hydrothermal process offers great opportunity for scale-up preparation of quasi one-dimensional materials of other chalcogenides.

The authors would like to acknowledge the financial supports of 863 Project (No 2001AA513023), the Natural Science Foundation of China (No 60225010) and the Zhejiang Provincial Natural Science Foundation of China (No 601092).

References

- [1] Agarwal A, Patel P D and Lakshminarayana D 1994 *J. Cryst. Growth* **142** 344
- [2] Lokhande C D 1990 *J. Phys. D: Appl. Phys.* **23** 703
- [3] Lotarski J J 1956 *J. Appl. Phys.* **27** 777
- [4] Chu D, Walser R M, Bene R W and Courtney T H 1974 *Appl. Phys. Lett.* **24** 479
- [5] Pahl S G and Fredgold R H 1971 *J. Pure Appl. Phys.* **4** 713
- [6] Price L S, Parkin I P, Hibben T G and Molloy K C 1998 *Chem. Vapor Depos.* **4** 222
- [7] Shibata T, Minra T, Kishi T and Nagai T 1990 *J. Cryst. Growth* **106** 593
- [8] Ghazali A, Zainal Z, Hussein M Z and Kassim A 1998 *Sol. Energy Mater. Sol. Cells* **55** 237
- [9] Nnebeony K W, Collins G E, Lee P A, Chau L K, Danziger J, Osburn E and Armstrong N R 1991 *Chem. Mater.* **3** 829
- [10] Getiz A and Lopez S 1994 *Semicond. Sci. Technol.* **9** 2130
- [11] Duan X, Huang Y, Agarwal K and Lieber C M 2003 *Nature* **421** 241
- [12] Fuhrer M S, Nygard J, Shih L, Furro M, Yoon Y G, Mazzoni M and Choi H J 2000 *Science* **288** 494
- [13] Ren Z F, Huang Z P, Xu J W, Wang J H, Bush P, Siegel M P and Provencio P N 1998 *Science* **282** 1105
- [14] Hai B, Tang K B, Wang C R, An C H, Yang Q, Shen G Z and Qian Y T 2001 *J. Cryst. Growth* **225** 92
- [15] An C H, Tang K B, Shen G Z, Wang C R, Yang Q, Hai B and Qian Y T 2002 *J. Cryst. Growth* **244** 333
- [16] Swayambanathan V, Hayes D, Schmidt K H, Liao Y X and Meisel D 1990 *J. Am. Chem. Soc.* **112** 3831
- [17] Hayes D, Meise O I, Nenadovic M T, Swayambanathan V and Meisel D 1989 *J. Phys. Chem.* **93** 4603
- [18] Zhang H, Ma X, Ji Y, Xu J and Yang D 2003 *Chem. Phys. Lett.* **377** 654
- [19] Zhang H, Ma X, Ji Y, Xu J and Yang D 2003 *Nanotechnology* **14** 974

temperatures. The nitride (TiN), and borides (TiB and TiB₂) are interstitial compounds that are very stable, hard, and refractory. Highly reflective, gold-colored TiN films can be made by chemical vapor deposition of TiCl₄(NH₃)₂.³

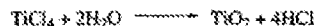
The metal is not attacked by mineral acids at room temperature or even by hot aqueous alkali. It dissolves in hot HCl, giving Ti^{III} species, whereas hot HNO₃ converts it into a hydrous oxide that is rather insoluble in acid or base. The best solvents are HF or acids to which fluoride ions have been added. Such media dissolve Ti and hold it in solution as fluoro complexes.

TITANIUM COMPOUNDS

17-A-2 The Chemistry of Titanium(IV), d⁰

Binary Compounds

Halides. The tetrachloride (TiCl₄), the usual starting point for the preparation of most other Ti compounds, is a colorless liquid (mp -23°C, bp 136°C) with a pungent odor. The Ti—Cl bond is short, 2.17 Å, possibly due to π donation $\text{Ti} \leftarrow \text{Cl}$. Titanium tetrachloride fumes strongly in moist air and is vigorously, though not violently, hydrolyzed by water:



With some HCl present or a deficit of H₂O, partial hydrolysis occurs, giving oxochlorides (see later).

Titanium tetrabromide⁴ and a metastable form of TiI₄ are crystalline at room temperature and are isomorphous with SiI₄, GeI₄, and SnI₄, having molecular lattices. The fluoride is obtained as a white powder by the action of F₂ on Ti at 200°C or by solvothermal decomposition of (O₂)₂Ti₂F₁₀; it sublimates readily and is hygroscopic; its structure is dominated by isolated columns of corner-linked TiF₆—octahedra.⁵ All the halides behave as Lewis acids; with neutral donors such as ethers they give adducts (see later).

Titanium Oxide;⁶ Complex Oxides; Sulfide. The naturally occurring dioxide TiO₂ has three crystal modifications, *rutile*, *anatase*, and *brookite*. In *rutile*, the commonest, the Ti is octahedral and this structure is a common one for MX₂ compounds. In *anatase* and *brookite* there are very distorted octahedra of oxygen atoms about each titanium, two being relatively close. Although *rutile* has been assumed to be the most stable form because of its common occurrence, *anatase* is 8 to 12 kJ mol⁻¹ more stable than *rutile*.

The dioxide is used as a white pigment.⁷ Naturally occurring forms are usually colored, sometimes even black, owing to the presence of impurities such as iron.

³C. H. Winter et al., *Inorg. Chem.* **1994**, *33*, 1227.

⁴S. I. Troyanov et al., *Russ. J. Inorg. Chem.* **1990**, *35*, 494.

⁵B. G. Müller et al., *Z. anorg. allg. Chem.* **1995**, *621*, 1227.

⁶K. I. Hadjivanov and G. Klissurski, *Chem. Soc. Rev.* **1996**, 61.

⁷A. Baidins et al., *Progr. Org. Coatings* **1992**, *20*, 105.

Pigment-grade material is generally made by hydrolysis of titanium(IV) sulfate solution or vapor-phase reaction of TiCl_4 with oxygen. The solubility of TiO_2 depends considerably on its chemical and thermal history. Strongly roasted specimens are chemically inert but under hydrothermal conditions they can be used to prepare zeolites.⁹ It reacts also with glycol in the presence of alkali metal hydroxides to yield soluble titanium glycolates.⁹ The dioxide impregnated with some metal complexes has been much studied as a catalyst for photodecomposition of water.¹⁰ Ultraviolet irradiation of a gas/solid interface of microcrystalline TiO_2 in the presence of H_2O and CO_2 leads to the formation of CO , H_2 , and CH_4 .¹¹ Many other uses are known; examples are found in catalysis¹² and preparation of devices such as film electrodes.¹³

Hydrous titanium dioxide is made by adding base to Ti^{IV} solutions and by action of acids on alkali titanates. The hydrous material dissolves in bases giving hydrous "titanates."

Many materials called "titanates" are known; nearly all have one of the three major mixed metal oxide structures. Indeed the names of two of the structures are those of the Ti compounds that were the first found to possess them, namely, *ilmenite* (FeTiO_3) and *perovskite* (CaTiO_3). Other titanites with the ilmenite structure are MgTiO_3 , MnTiO_3 , CoTiO_3 , and NiTiO_3 , and others with the perovskite structure are SrTiO_3 and BaTiO_3 . There are also titanates with the spinel structure such as Mg_2TiO_4 , Zn_2TiO_4 , and Co_2TiO_4 . The Li_2TiO_4 is isostructural with Li_2GeO_4 and contains tetrahedrally coordinated Ti^{IV} ions and tetragonally packed oxide ions;¹⁴ $\text{Rb}_2\text{NaTiO}_4$ is isotypic with $\text{Rb}_2\text{NaPbO}_4$.¹⁵

Barium oxide and TiO_2 react to form an extensive series of phases from simple ones such as BaTiO_3 (commonly called barium titanate) and Ba_2TiO_4 to $\text{Ba}_4\text{Ti}_{13}\text{O}_{36}$ and $\text{Ba}_6\text{Ti}_7\text{O}_{28}$, the general formula being $\text{Ba}_x\text{Ti}_y\text{O}_{x+2y}$. All are of technical interest because of their ferroelectric properties, which may be qualitatively understood as follows. The Ba^{2+} ion is so large relative to the small ion Ti^{4+} that the latter can literally "rattle around" in its octahedral hole. When an electric field is applied to a crystal of this material, it can be highly polarized because each of the Ti^{4+} ions is drawn over to one side of its octahedron, thus causing an enormous electrical polarization of the crystal as a whole.

Titanium disulfide, like the disulfides of Zr, Hf, V, Nb, and Ta, has a layer structure; two adjacent close-packed layers of S atoms have Ti atoms in octahedral interstices. These "sandwiches" are then stacked so that there are adjacent layers of S atoms. Lewis bases such as aliphatic amines can be intercalated between these adjacent sulfur layers; similar intercalation compounds can be made with MS_2 and MSe_2 compounds for $\text{M} = \text{Ti}$, Zr, Hf, V, Nb, and Ta. Many of these have potentially useful electrical properties, including use as cathode material for lithium batteries, and superconductivity, and may be compared with the intercalation compounds of

⁹X. Liu and J. K. Thomas, *J. Chem. Soc., Chem. Commun.* **1996**, 1435.

¹⁰L. Lensink et al., *Inorg. Chem.* **1995**, *34*, 746.

¹¹See for example: J. T. Yates, Jr. et al., *Chem. Rev.* **1995**, *95*, 735.

¹²I. Kamber et al., *J. Chem. Soc., Chem. Commun.* **1995**, 533.

¹³K. I. Hadjiivanov and D. G. Klissurski, *Chem. Soc. Rev.* **1996**, 61.

¹⁴T. Gorfín et al., *Prog. Inorg. Chem.* **1997**, *44*, 345.

¹⁵R. P. Gunawardane et al., *J. Solid State Chem.* **1994**, *112*, 70.

¹⁶C. Weiss and R. Hoppe, *Z. anorg. allg. Chem.* **1996**, *622*, 603.

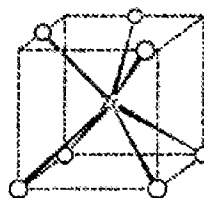
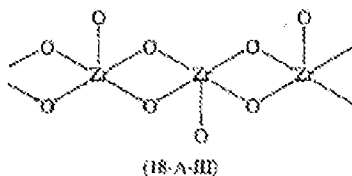


Figure 18-A-2 Coordination geometry in the baddeleyite form of ZrO_2 .

Zirconium Oxide and Mixed Oxides

Addition of hydroxide to zirconium(IV) solutions causes the precipitation of white gelatinous $\text{ZrO}_2 \cdot n\text{H}_2\text{O}$, where the water content is variable. On strong heating, this hydrous oxide gives hard, white, insoluble ZrO_2 .¹¹ This has an extremely high melting point (2700°C), exceptional resistance to attack by both acids and alkalis, and good mechanical properties; it is used for crucibles and furnace cores. Zirconium dioxide in its monoclinic (baddeleyite) form and one form of HfO_2 are isomorphous and have a structure in which the metal atoms are 7-coordinate, as shown in Fig. 18-A-2. Three other forms of ZrO_2 have been described, but none has the rutile structure so often found among MO_2 compounds.

A number of compounds called “zirconates” may be made by combining oxides, hydroxides, nitrates, and so on, of other metals with similar zirconium compounds and firing the mixtures at 1000 to 2500°C . These, like their titanium analogues, are mixed metal oxides; there are no discrete zirconate ions known. The zirconate CaZrO_3 is isomorphous with perovskite. By dissolving ZrO_2 in molten KOH and evaporating off the excess of solvent at 1050°C , the crystalline compounds $\text{K}_2\text{Zr}_2\text{O}_5$ and K_2ZrO_3 may be obtained. The former contains ZrO_4 octahedra sharing faces to form chains that in turn share edges and corners with other chains. The latter contains infinite chains of ZrO_3 square pyramids (18-A-III).



The other chalcogenides, ZrE_2 and HfE_2 ($\text{E} = \text{S}, \text{Se}, \text{and Te}$) have layered structures and are intrinsic semiconductors. They can also form intercalation compounds which generally have layered structures.

Aqueous Chemistry

This is not very extensive because a $+4$ ion, even a large one, tends to be extensively hydrolyzed. Only at very low concentration ($\sim 10^{-4} \text{ M}$) and high acidity ($[\text{H}^+]$ of $1\text{--}2 \text{ M}$) does the $\text{Zr}^{4+}(\text{aq})$ ion appear to exist. Zirconium dioxide is more basic than TiO_2 and is virtually insoluble in excess base. No ZrO^{2+} ion has been detected

¹¹See for example: E. Kato et al., *J. Mater. Sci.* **1997**, 32, 1789.